

Synchronization stability between initial-dependent oscillators with periodical and chaotic oscillation^{*}

Fu-qiang WU¹, Jun MA^{†‡1,2,3}, Guo-dong REN¹

¹Department of Physics, Lanzhou University of Technology, Lanzhou 730050, China

²School of Science, Chongqing University of Posts and Telecommunications, Chongqing 430065, China

³NAAM-Research Group, Department of Mathematics, King Abdulaziz University, Jeddah, Saudi Arabia

[†]E-mail: hyperchaos@163.com

Received May 28, 2018; Revision accepted June 8, 2018; Crosschecked June 13, 2018; Published online July 28, 2018

Abstract: The selection of periodical or chaotic attractors becomes initial-dependent in that setting different initial values can trigger a different profile of attractors in a dynamical system with memory by adding a nonlinear term such as z^2y in the Rössler system. The memory effect means that the outputs are very dependent on the initial value for variable z , e.g. magnetic flux for a memristor. In this study, standard nonlinear analyses, including phase portrait, bifurcation analysis, and Lyapunov exponent analysis were carried out. Synchronization between two coupled oscillators and a network was investigated by resetting initial states. A statistical synchronization factor was calculated to find the dependence of synchronization on the coupling intensity when different initial values were selected. Our results show that the dynamics of the attractor depends on the selection of the initial value for one variable z . In the case of coupling between two oscillators, appropriate initial values are selected to trigger two different nonlinear oscillators (periodical and chaotic). Results show that complete synchronization between periodical oscillators, chaotic oscillators, and periodical and chaotic oscillators can be realized by applying an appropriate unidirectional coupling intensity. In particular, two periodical oscillators can be coupled bidirectionally to reach chaotic synchronization so that periodical oscillation is modulated to become chaotic. When the memory effect is considered on some nodes of a chain network, enhancement of memory function can decrease the synchronization, while a small region for intensity of memory function can contribute to the synchronization of the network. Finally, dependence of attractor formation on the initial setting was verified on the field programmable gate array (FPGA) circuit in digital signal processing (DSP) builder block under Matlab/Simulink.

Key words: Synchronization; Bifurcation; Synchronization factor; Field programmable gate array (FPGA)
<https://doi.org/10.1631/jzus.A1800334>

CLC number: O59; TN710


1 Introduction

In recent decades, the potential applications of chaotic systems have been investigated. Chaotic systems have some distinct characteristics, for example, the occurrence of strange attractors, sensitivity to initial values, wide frequency scope, and at least one

positive Lyapunov exponent (Fixman, 1984; Vaidyanathan and Volos, 2016). Deterministic chaos denotes irregular or chaotic motion confirmed using high speed computers and refined experimental techniques. Dynamical systems composed of deterministic chaos are classified as dissipative and divergent systems (Honein et al., 1991; Sieberer et al., 2013; Ruggieri and Speciale, 2017). Chaos can be triggered in many nonlinear dynamical systems in many different ways. For example, a simple oscillator (pendulum) driven by periodical forcing can present switches between regular and chaotic motion (Luo and Han, 2000; Luo and Min, 2011). In the Rayleigh-Benard experiment (Martinet and Adrian, 1988) a

[‡] Corresponding author

^{*} Project supported by the National Natural Science Foundation of China (Nos. 11765011 and 11672122)

 ORCID: Fu-qiang WU, <https://orcid.org/0000-0002-3850-7400>; Jun MA, <https://orcid.org/0000-0002-6127-000X>

© Zhejiang University and Springer-Verlag GmbH Germany, part of Springer Nature 2018

transition was observed from periodic to chaotic motion by analyzing the power spectrum. Belousov-Zhabotinsky (Györgyi and Field, 1992) studied chaotic motion in chemical reaction processes. Understanding the main properties of chaos can give guidance for its potential applications, for example, chaos-based secure communication (Carroll and Pecora, 1993; Lau and Tse, 2003). However, chaotic motion in a washing machine or other household appliances could cause damage to these machines, so some feasible schemes have been proposed to suppress and control chaos in chaotic systems so that they maintain their stability. The well-known scalar driving method (Peng et al., 1996; Chen et al., 2004), coupling control (Heagy et al., 1995), and the impulsive-control method (Yang et al., 1997) are effective for controlling chaos in low-dimensional dynamical systems. Synchronization is a common phenomenon in nature, and is often produced in networks composed of nonlinear oscillators. The first empirical evidence for this was observed by Huygens who showed chocks hanging from the same wooden rod reached synchronization (Pena Ramirez et al., 2013). Yamada and Fujisaka (1986) discovered an unusual type of intermittent behavior in coupled identical chaotic systems. An intermittent synchronization is reached between neurons with electromagnetic induction (Ma et al., 2017c). The synchronous stability of the two coupled Rössler models was investigated by approximating the trajectory (Cheng and Chen, 2017). Switched synchronization was confirmed in a class of chaotic systems with multiple delays by using a periodically intermittent control (Liu et al., 2016). Practical applications of synchronization began to attract interest following experimental implementations based on field programmable gate array (FPGA) (Giordano and Aloisio, 2011).

In recent decades, synchronization among chaotic systems has been investigated extensively (Hu et al., 1997; Li et al., 2008; Pecora and Carroll, 2015). Many types of synchronization have been confirmed in dynamical systems, including complete synchronization (Lin and He, 2005; Mahmoud and Mahmoud, 2010), phase synchronization (Osipov et al., 2002; Ma et al., 2011, 2017b), and generalized synchronization (Hunt et al., 1997; Yang and Duan, 1998). Chaotic properties are often observed in the electrical activities of neurons, and the stability of

synchronization between neurons is of interest because it can give guidance in understanding the occurrence of neuronal diseases such as seizures. Synchronization has been investigated in two neurons with asymmetric-structured electric coupling (Wang et al., 2018). For chaotic circuits, voltage coupling via resistance is often applied to bridge two chaotic systems and change the dynamical response of chaotic circuits (Ueda and Akamatsu, 1981; Anshan, 1988). For signals sampled from the nervous system or brain, chemical and electrical synapses are effective for encoding information and connect different neurons for signal exchange (Graubard and Hartline, 1987; Friedman and Strowbridge, 2003; Pereda, 2014). Synchronization and information encoding via chemical or electrical synapses can be detected in neurons (Podvigin et al., 2008; Wang et al. 2011). These results are helpful for understanding the pathogenesis, progress, and prognosis of diseases, and provide guidance for the prevention of epilepsy and Parkinson's disease (Szot, 2012; Vyas et al., 2016). Multi-agent and biological systems often contain a large number of agents or cells. Mode transition in their collective behavior can be described using networks or coupled oscillators with an appropriate connection type. For example, collective behavior has been described in an improved neuronal model considering the effect of electromagnetic induction (Xu et al., 2017; Zhang and Liu, 2018). Pattern development and dynamics in cardiac tissue exposed to electromagnetic radiation has been investigated by setting different initial states (Wu et al., 2016, 2017). These results account for two different death mechanisms of the heart due to electromagnetic radiation. In most previous studies, time delay was often introduced to describe the memory effect. However, magnetic flux across a memristor and memory function (Lv et al., 2016; Wang et al., 2017; Mankin et al., 2018) throw light on understanding the nonlinear properties of dynamical systems. For example, a generic dynamical system (Ma et al., 2017a) has been proposed to realize a switch between chaotic and periodic states by resetting the initial values for variables even when all parameters are fixed. It would be helpful to trigger more reliable and secure key series for secure communication. Therefore, it is important to investigate the synchronization dependence and stability of these initial-dependent dynamical systems with memory.

In recent decades, chaos-based problems have been extensively investigated in analog circuits and dynamical models. It is more attractive and important to explore the use of embedded systems for the implementation of chaotic systems, such as the application of FPGA to secure communication and dynamical simulation (Tlelo-Cuautle et al., 2016b, 2017; Pano-Azucena et al., 2017). In this study, the dynamical response and synchronization problem are investigated in an emanative dynamical system with memory, which adds the nonlinear term z^2y to the Rössler system. The factor of synchronization is calculated to analyze the synchronization transition, and then the part of the implementation based on FPGA (Trejo-Guerra et al., 2012; Tlelo-Cuautle et al., 2015b, 2016c) is verified to find the dependence on the initial selection of variables.

2 Model descriptions

The Rössler system (Rössler, 1976) contains three variables and is described by three ordinary differential equations. An emanative dynamical system can present periodic, stable, and chaotic states by setting appropriate parameters. The use of nonlinear circuits composed of memristors by Ma et al. (2017a) suggested that the Rössler system could be improved by adding new nonlinear terms. Thus, periodic and chaotic states could be selected arbitrarily by resetting the initial values. The improved three-variable system is described by

$$\begin{cases} \frac{dx}{dt} = -y - z, \\ \frac{dy}{dt} = x + ay - kz^2y, \\ \frac{dz}{dt} = b + z(x - c), \end{cases} \quad (1)$$

where x , y , and z are variables in the oscillator model. The parameters were selected as $a=0.38$, $b=0.2$, $c=5.6$, and $k=0.6$. Chaotic series are detected from Eq. (1) when the quadratic nonlinearity kz^2y is removed ($k=0$). Due to activation of the nonlinear term kz^2y , Eq. (1) becomes more sensitive to the initial setting for variable z (Ma et al., 2017a). The potential mechanism could be that kz^2 can be thought of as a time-varying

feedback parameter for variable y , such that a slight difference in the initial setting will trigger a different parameter region. When variable z is thought of as magnetic flux, kz^2y is regarded as an induction current while variable y is regarded as the voltage on a capacitor in the circuit. First, we discuss the synchronization approach between two identical oscillators with memory, calculating unidirectional and bidirectional coupling:

$$\begin{cases} \frac{dx_1}{dt} = -y_1 - z_1 + g'_x(x_2 - x_1), \\ \frac{dy_1}{dt} = x_1 + ay_1 - kz_1^2y_1 + g'_y(y_2 - y_1), \\ \frac{dz_1}{dt} = b + z_1(x_1 - c) + g'_z(z_2 - z_1), \end{cases} \quad (2a)$$

$$\begin{cases} \frac{dx_2}{dt} = -y_2 - z_2 + g_x(x_1 - x_2), \\ \frac{dy_2}{dt} = x_2 + ay_2 - kz_2^2y_2 + g_y(y_1 - y_2), \\ \frac{dz_2}{dt} = b + z_2(x_2 - c) + g_z(z_1 - z_2), \end{cases} \quad (2b)$$

where g_x , g_y , g_z , g'_x , g'_y , and g'_z describe the coupling intensity between variables, and $g'_x=g'_y=g'_z=0$ indicates a unidirectional coupling type. At the same time, the pattern of synchronization is investigated under different initial state settings. The collective behavior and dynamics in the chain network are discussed and the dynamical equations coupled by the second variable are described as follows:

$$\begin{cases} \frac{dx_i}{dt} = -y_i - z_i, \\ \frac{dy_i}{dt} = x_i + ay_i - k_i z_i^2 y_i + g_y(y_{i+1} + y_{i-1} - 2y_i), \\ \frac{dz_i}{dt} = b + z_i(x_i - c), \end{cases} \quad (3)$$

where the subscript i is the node position of the chain network. g_y denotes the coupling intensity between adjacent oscillators in the network. The parameters were fixed at $a=0.38$, $b=0.2$, $c=5.6$, and $k=0.6$. To discern the collective behavior and degree of synchronization, a statistical factor R (Wang and Ma, 2018) was introduced using the mean field theory:

$$R = \frac{\langle F^2 \rangle - \langle F \rangle^2}{\frac{1}{N} \sum_{i=1}^N \langle x_i^2 \rangle - \langle x_i \rangle^2}, \quad F = \frac{1}{N} \sum_{i=1}^N x_i, \quad (4)$$

where N denotes the number of nodes, and the symbol $\langle \cdot \rangle$ is the average calculation over time. The synchronization factor $R \sim 1$ means that the chain network presents perfect synchronization, while non-perfect synchronization is reached at $R \sim 0$. For pattern selection and formation, a smaller factor of synchronization is helpful to develop a regular spatial distribution.

3 Numerical results and discussion

In the numerical studies, the fourth-order Runge-Kutta algorithm was used in MatlabR2014 with time step $h=0.01$. First, initial values were selected as $(x_0, y_0, z_0) = (0.0, 0.0, \#)$. The nonlinear properties of Eq. (1) are very dependent on the feedback k in the quadratic

nonlinear terms z^2y , and slight variation in the initial value z_0 can result in distinct diversity in the profile of attractors and orbits (Fig. 1).

Fig. 1 shows that the attractor profile is highly dependent on the initial value, and transition from a chaotic to a periodical state is triggered by changing the initial values to $z_0 = [-6.0, 6.0]$. The selection of the attractor profile is not a monotonous transition from a chaotic to a periodical state with an increasing initial setting value z_0 . Furthermore, sampled time series from the first variable were calculated for bifurcation analysis, and the largest Lyapunov exponent was calculated to determine how the chaos region is dependent on the initial value z_0 (Fig. 2).

Fig. 2 shows that the transition between periodical and chaotic states can be induced by increasing the initial intensity z_0 . The distribution of the largest Lyapunov exponents confirmed that an appropriate setting for the initial variable z can enhance the occurrence of chaos, while periodical or weak chaos can be triggered at $z_0 = -3.0, -1.0, 2.0, 6.0$. As a result,

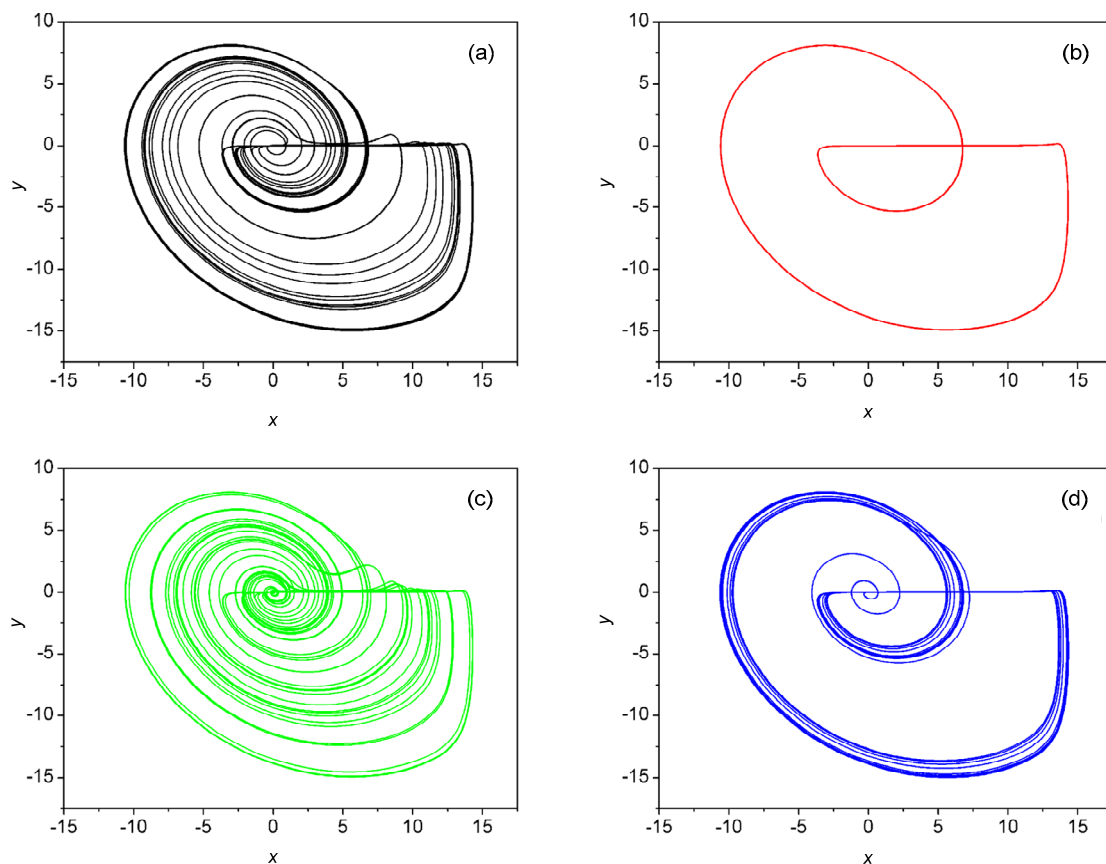


Fig. 1 Phase portraits calculated to find the dependence of attractors on the initial setting value z_0 with fixed parameters $a=0.38$, $b=0.2$, $c=5.6$, and $k=0.6$, for (a) $z_0=-6.0$; (b) $z_0=-3.3$; (c) $z_0=0.0$; (d) $z_0=2.1$

different oscillations are induced when oscillators are endowed with different initial values. Therefore, synchronization involves different cases: periodical vs. periodical, periodical vs. chaotic, and chaotic vs. chaotic states (CS). That is, in the case of synchronization between two oscillators, diversity in the initial setting z_0 will determine whether oscillators are identical or non-identical. The error function between two coupled oscillators is calculated by

$$D(t) = \sqrt{(x_2 - x_1)^2 + (y_2 - y_1)^2 + (z_2 - z_1)^2}. \quad (5)$$

Parameters and initial values were carefully selected to trigger two chaotic oscillators. Unidirectional coupling was applied to determine the stability of synchronization between the chaotic oscillators, then the attractor profile and evolution of error function were calculated (Fig. 3).

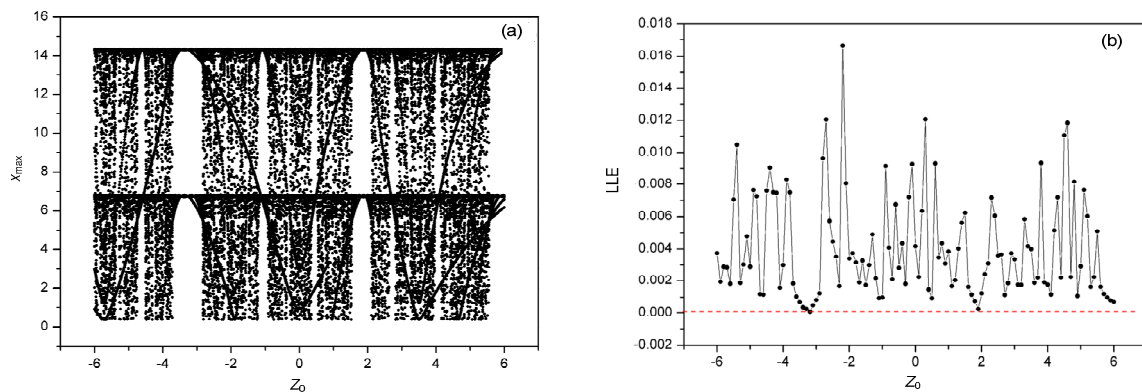


Fig. 2 Bifurcation diagram for the maximal variable x , x_{\max} (a) and the largest Lyapunov exponent (LLE) (b) after applying different initial values of z_0 , with parameters set as $a=0.38$, $b=0.2$, $c=5.6$, and $k=0.6$

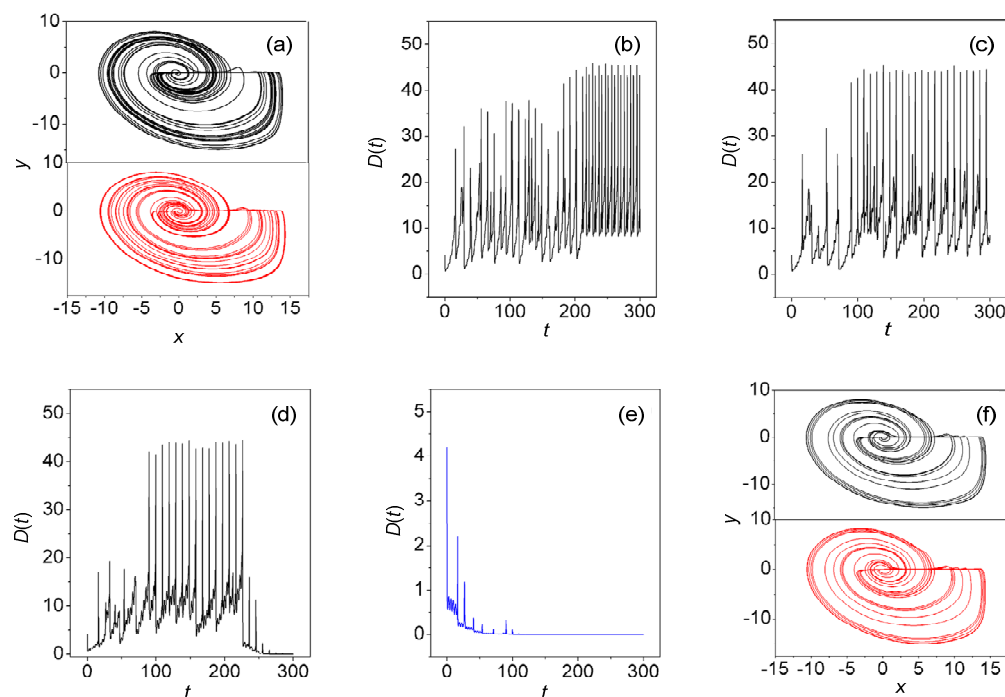


Fig. 3 Evolution of the error function, Eq. (5), and chaotic attractors for the drive and response system were calculated by setting different gains g_x under unidirectional coupling

The parameters were selected as $a=0.38$, $b=0.2$, $c=5.6$, $k=0.6$, and $g'_x=g'_y=g'_z=g_y=g_z=0.0$. Initial values were selected as $[0.0, 0.0, 0.3]$, $[0.0, 0.0, 4.5]$, for (a) starting state; (b) $g_x=0.0$; (c) $g_x=0.1$; (d) $g_x=0.2$; (e) $g_x=0.4$; (f) synchronization between chaotic attractors at $g_x=0.4$

The results shown in Fig. 3 confirmed that complete synchronization can be realized between two identical chaotic oscillators by applying an appropriate coupling gain via the variable x . The strange attractors become the same under unidirectional coupling. The same calculation was carried out on two periodical oscillators, and periodical synchronization (PS) was investigated (Fig. 4).

Similarly, the results in Fig. 4 show that complete synchronization is achieved by setting an appropriate unidirectional coupling gain. Furthermore, it is important to discuss the case for synchronization between a periodical oscillator and a chaotic oscillator. For simplicity, the driving system was triggered as periodical oscillation, the response or driven system was designed to have chaotic oscillation behavior, then unidirectional coupling was switched on. It is important to estimate the synchronization and whether chaotic or periodical synchronization is reached. The results are shown in Fig. 5.

The results in Fig. 5 show that the chaotic oscillator was suppressed to generate periodical oscillation.

When unidirectional coupling from the periodical oscillator began to activate the response system, then the chaotic oscillator was tamed to a periodical state. Finally, two periodical oscillators achieved complete synchronization. The potential mechanism is that periodical forcing from the driving system (periodical oscillator) imposes a continuous periodical stimulus. Thus, the response system has to keep pace with the driving system with the same rhythm. A larger coupling intensity is known to be more effective to realize synchronization between oscillators.

We investigated three cases each with a different synchronization approach: synchronization of PS, synchronization of chaotic oscillators (COS), and synchronization between a periodical oscillator and a chaotic oscillator (PC). The results for the coupling threshold detected for the synchronization approach under the three cases are shown in Fig. 6.

The results confirmed that unidirectional coupling is effective in stabilizing synchronization with increasing coupling intensity, and the error function decreases to zero within a transient period. Among

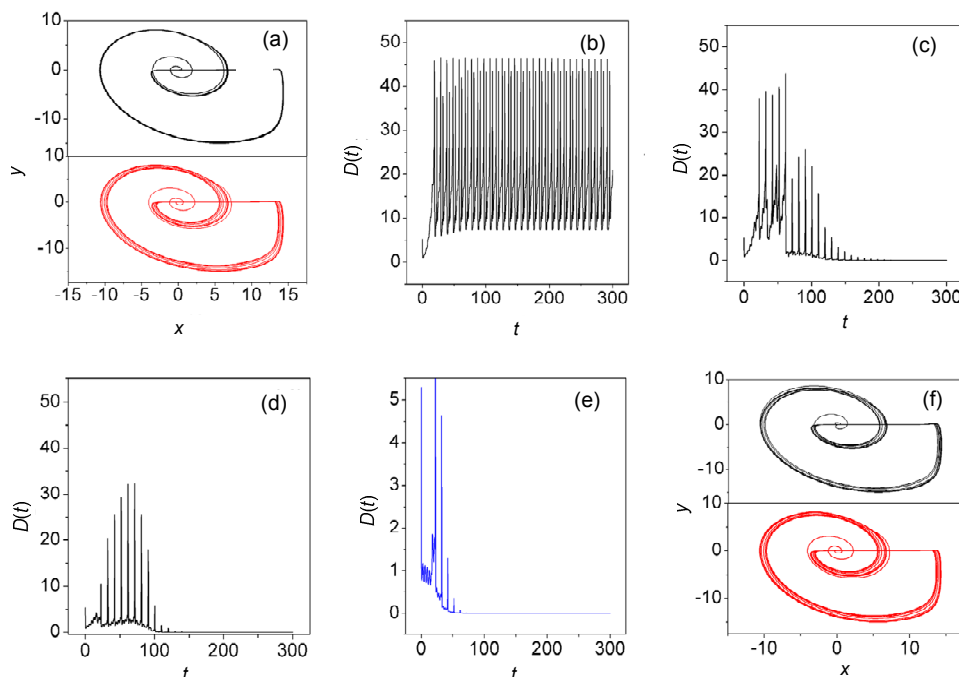


Fig. 4 Evolution of the error function Eq. (5) and periodical attractors for the drive and response system were calculated by setting different gains g_x under unidirectional coupling

The parameters were selected as $a=0.38$, $b=0.2$, $c=5.6$, $k=0.6$, and $g'_x=g'_y=g'_z=g_z=0.0$; initial values as $[0.0, 0.0, -3.2]$, $[0.0, 0.0, 2.1]$, for (a) starting state; (b) $g_x=0.0$; (c) $g_x=0.1$; (d) $g_x=0.2$; (e) $g_x=0.4$; (f) synchronization between periodical attractors at $g_x=0.4$

the three cases, coupling between periodical and chaotic oscillators seemed to have a lower threshold for coupling intensity under synchronization. The other two cases needed an increase in coupling intensity even when the same parameters were fixed. A periodical oscillator often holds distinct periodicity and remains resistant to external forcing, while periodical forcing or modulation is effective in taming chaotic oscillation due to forced vibration.

Bidirectional coupling between oscillators and neurons can enhance consensus and synchronization approach because each agent is self-adaptive in keeping pace with other agents. Therefore, the same case was under consideration when bidirectional coupling was applied to periodical and/or chaotic oscillators. The results are shown in Fig. 7.

Bidirectional coupling can enhance the synchronization approach. Both periodical oscillators

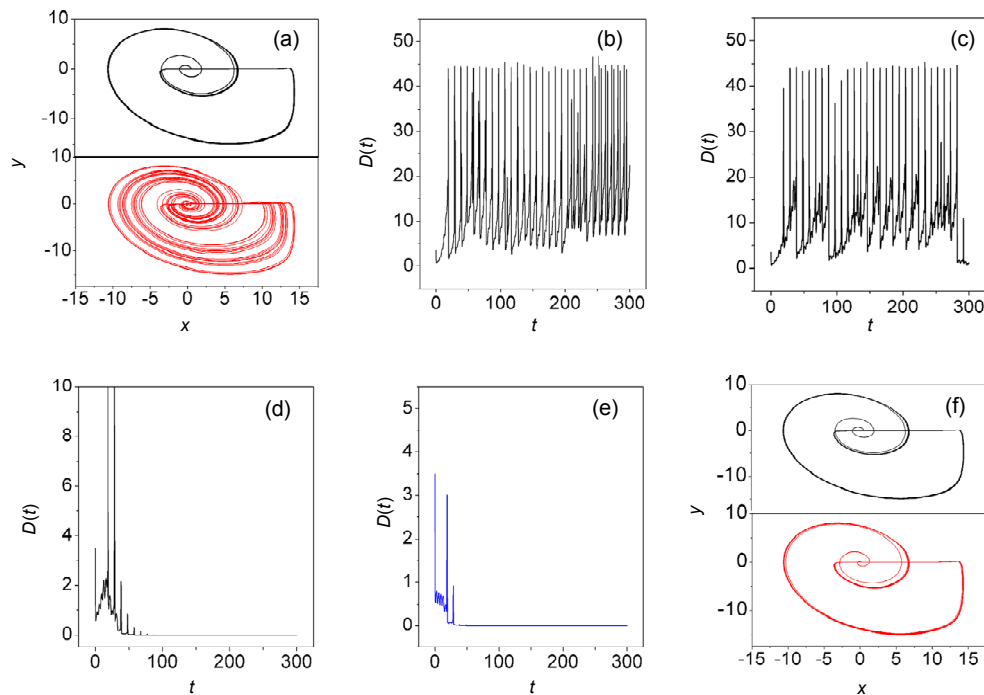


Fig. 5 Evolution of the error function Eq. (5) and periodical-chaotic attractors for the drive and response system were calculated by setting different gains g_x under unidirectional coupling

The parameters were selected as $a=0.38$, $b=0.2$, $c=5.6$, $k=0.6$, and $g'_x=g'_y=g'_z=g_y=g_z=0.0$; initial values as $[0.0, 0.0, -3.2]$, $[0.0, 0.0, 0.3]$, for (a) starting state; (b) $g_x=0.0$; (c) $g_x=0.1$; (d) $g_x=0.2$; (e) $g_x=0.4$; (f) synchronization of attractors

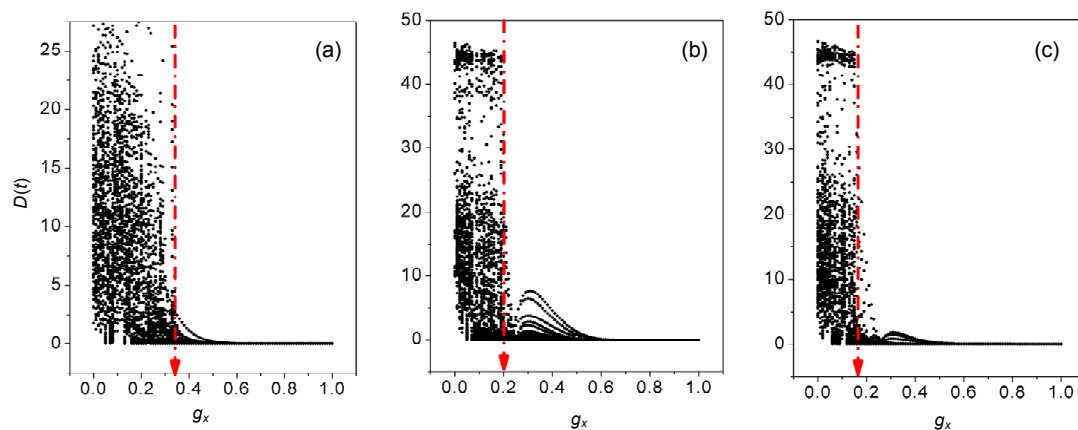


Fig. 6 Evolution of the error function Eq. (5) was calculated by setting different unidirectional coupling intensities g_x

The parameters were set as $a=0.38$, $b=0.2$, $c=5.6$, $k=0.6$, and $g'_x=g'_y=g'_z=g_y=g_z=0.0$; for (a) COS; (b) PS; (c) PC

were coupled to become chaotic after synchronization. Furthermore, the second variable y and third variable z are considered under bidirectional coupling. The dependence of the synchronization approach on coupling intensity when initial states were selected as $[0.0, 0.0, 0.3]$, $[0.0, 0.0, 4.5]$ is shown in Fig. 8.

Synchronization could be realized via coupling on x and y . However, complete synchronization was not reached under bidirectional coupling via z . The potential mechanism could be that the phase orbit and

attractor are highly dependent on the initial setting for z , and a slight difference in z may cause more diversity in orbits, thus making synchronization difficult. To further investigate the collective behaviors, a chain network was designed such that each oscillator connected to two adjacent oscillators, and a periodical boundary condition was used. For simplicity, the initial values were selected to trigger a chaotic oscillator, and variable y was used to bridge bidirectional coupling. Pattern evolution and the synchronization

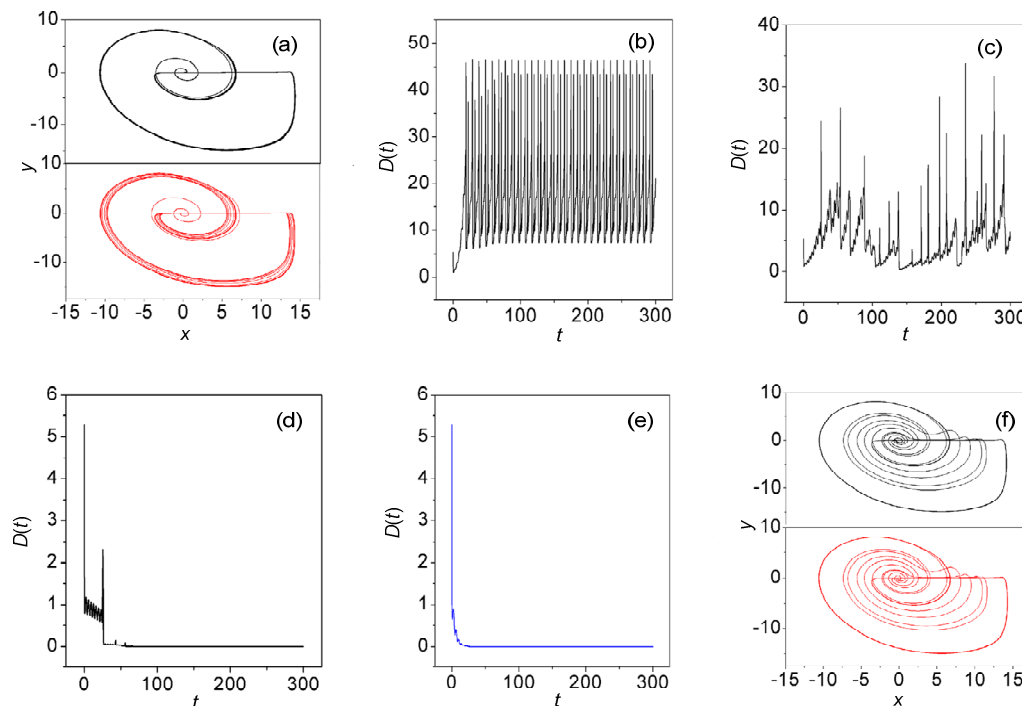


Fig. 7 Evolution of the error function Eq. (4) was calculated by setting a different gain g_x when the bidirectional coupling via variable x was adopted at fixed parameters $a=0.38$, $b=0.2$, $c=5.6$, and $k=0.6$; initial values were $[0.0, 0.0, -3.2]$, $[0.0, 0.0, 2.1]$, for (a) starting state; (b) $g_x=0.0$; (c) $g_x=0.1$; (d) $g_x=0.2$; (e) $g_x=0.4$; (f) final state

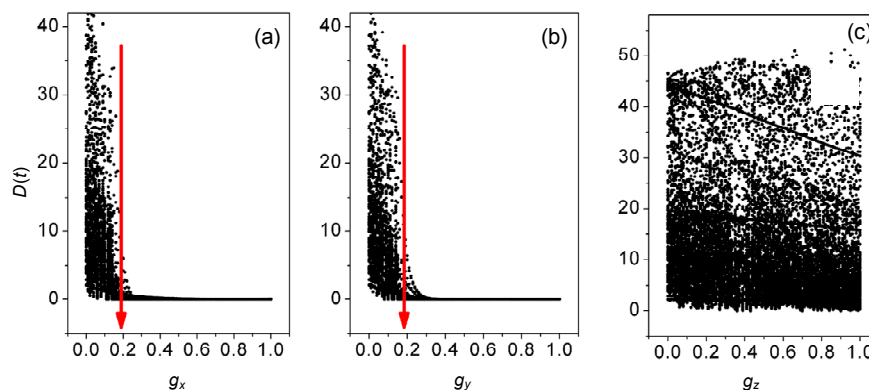


Fig. 8 Evolution of the dependence of the error function on bidirectional coupling intensity was calculated when initial values were selected to trigger chaotic oscillation

Parameters were set as $a=0.38$, $b=0.2$, $c=5.6$, and $k=0.6$ for (a) x -coupling; (b) y -coupling; (c) z -coupling

factor were plotted when a few oscillators ($i=3, 4, 5, 95, 96, 97$) were driven by the nonlinear memory term kz^2y , while other oscillators are described by the original Rössler model without a memory effect ($k=0$ in Eq. (1)). The initial values for the variables were selected as $(0.0, 0.0, 0.1 \times \text{random})$, and a random value was triggered in the scope $[0, 1]$. The development of a spatial pattern and factors of synchronization is plotted in Fig. 9.

The degree of synchronization improved and the factor of synchronization increased with increasing coupling intensity between oscillators of the chain

network. As a result, collective behavior in the network could present a regular spatial pattern when some nodes were considered with memory. When the memory term kz^2y was introduced into some oscillators ($i=3, 4, 5, 95, 96, 97$), heterogeneity was generated to trigger a continuous pulse that regulated the network. Extensive numerical results confirmed that the outputs of each oscillator will increase rapidly when all nodes (oscillators) are considering a memory term, and the network is cracked beyond numerical solution. Furthermore, the coupling intensity was fixed at $g_y=4.0$, and the feedback gain k in the memory term kz^2y on

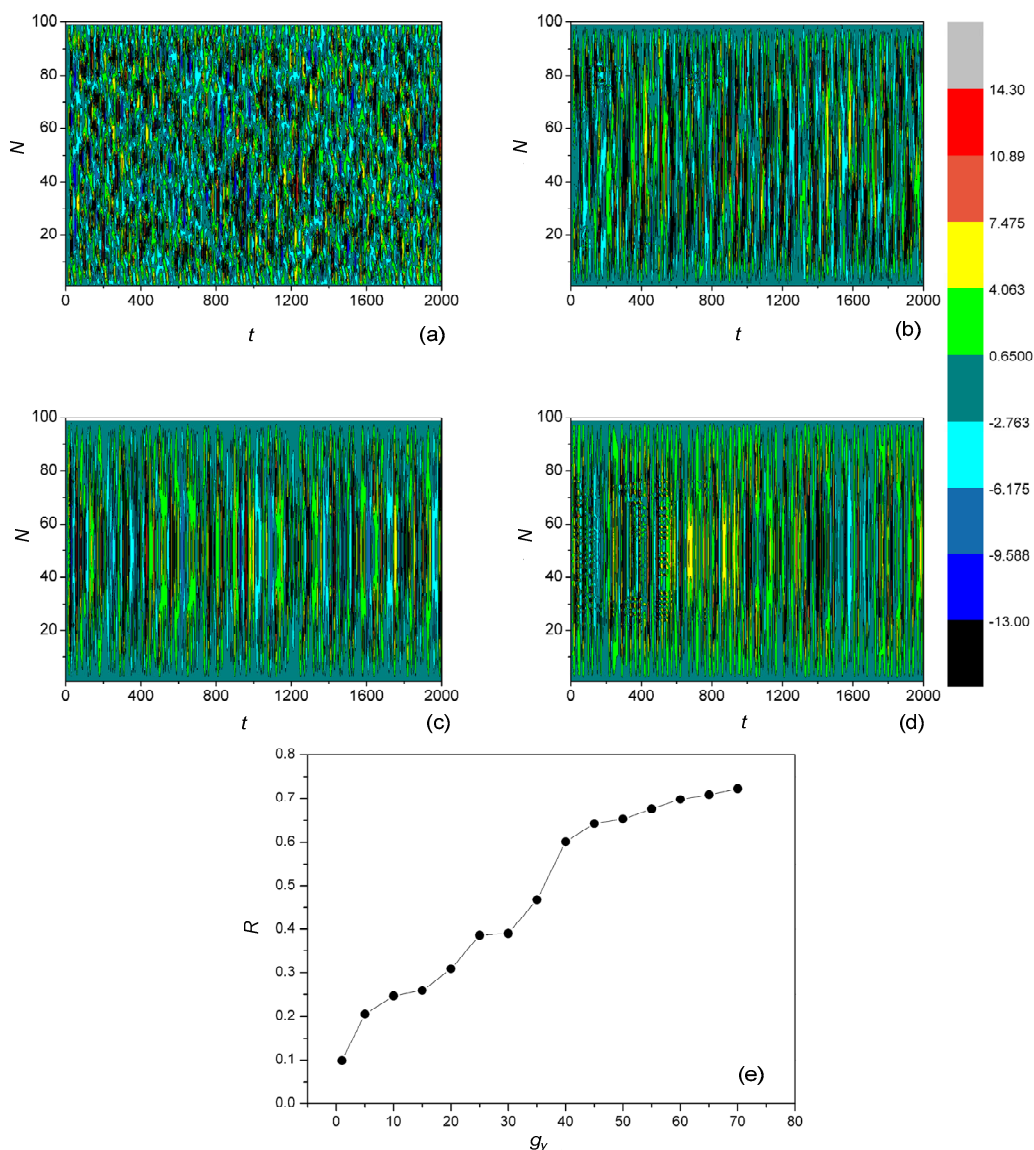


Fig. 9 Spatiotemporal evolution of a chain network coupled via variable y . Parameters were selected as $a=0.38$, $b=0.2$, $c=5.6$, $k_i=0.6$, and the bidirectional coupling intensity were (a) $g_y=0.01$; (b) $g_y=25$; (c) $g_y=50$; (d) $g_y=70$. Snapshots are shown in color scale by plotting the value for variable x . (e) shows the distribution for synchronization factor

Note: for interpretation of the references to color in this figure legend, the reader is referred to the web version of this article

some nodes was adjusted to find the synchronization approach. The results are plotted in Fig. 10.

The synchronization factor showed a slight dependence on feedback gain in the memory term, and a smaller coupling intensity g_y was insufficient to realize synchronization on the network. Comparing these results with previous conclusions, the improved Rössler with memory was highly dependent on the initial value setting of variable z , and different oscillators were activated and triggered when random initials were selected for each oscillator. As a result, it became difficult for the network to reach synchronization between non-identical oscillators, even though the coupling intensity increased greatly. New effective schemes are needed to overcome synchronization problems on this kind of network, composed of oscillators with memory.

4 Circuit implementation based on FPGA

Based on the improved Rössler model, dynamical behavior was investigated by resetting variant initial values for variable z . FPGA verification of chaotic systems is known to be useful for synthesizing architectures for potential applications (Trejo-Guerra et al., 2013; Tlelo-Cuautle et al., 2015a, 2016a). The circuit was designed by employing the FPGA circuit in digital signal processing (DSP) builder block under Matlab/Simulink. A diagram of the circuit implemented is shown in Fig. 11.

The circuit was activated to verify whether the formation of attractors was dependent on the setting of the initial value for z . The initial values for the first and second variables (x, y) were selected to be the same case as $(x_0, y_0)=(0.0, 0.0)$. A chaotic attractor

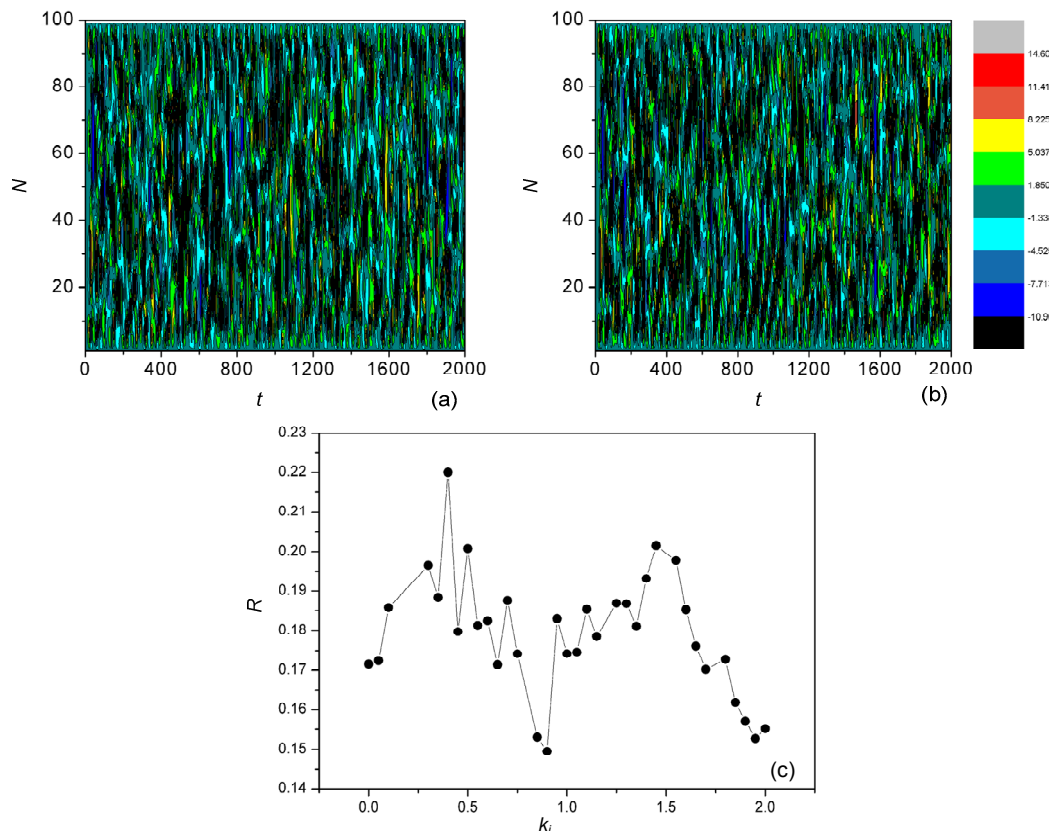


Fig. 10 Spatiotemporal evolution of a chain network (a, b) and the distribution for factors of synchronization (c) are plotted with fixed parameters of $a=0.38$, $b=0.2$, $c=5.6$, and $g_y=4.0$. The memory term $k_z z^2 y$ was considered on nodes ($i=3, 4, 5, 95, 96, 97$) for (a) $k_f=0.4$; (b) $k_f=0.9$. Snapshots are shown in color scale by plotting the value for variable x . (c) shows the distribution for synchronization factor

Note: for interpretation of the references to color in this figure legend, the reader is referred to the web version of this article

and periodical attractor can be obtained by using a digital platform. The results are shown in Fig. 12.

The improved Rössler model with memory could be verified to generate chaotic and/or periodical oscillation, and appropriate attractors could be formed by setting appropriate initial values for the variable z . This circuit could be further used to trigger chaotic series for secure communication, and intermittent resetting of the initial values could enhance

the safety of secure keys. Temperature and other variations like device parameters and initial conditions of chaotic systems can vary to induce mode transition or breakdown (de la Fraga and Tlelo-Cuautle, 2014), therefore, robust control becomes critical to finding the most optimal scheme. It is also useful to investigate the synchronization problems on oscillators with mixed modes of oscillation by choosing FPGA as the platform and the Xilinx

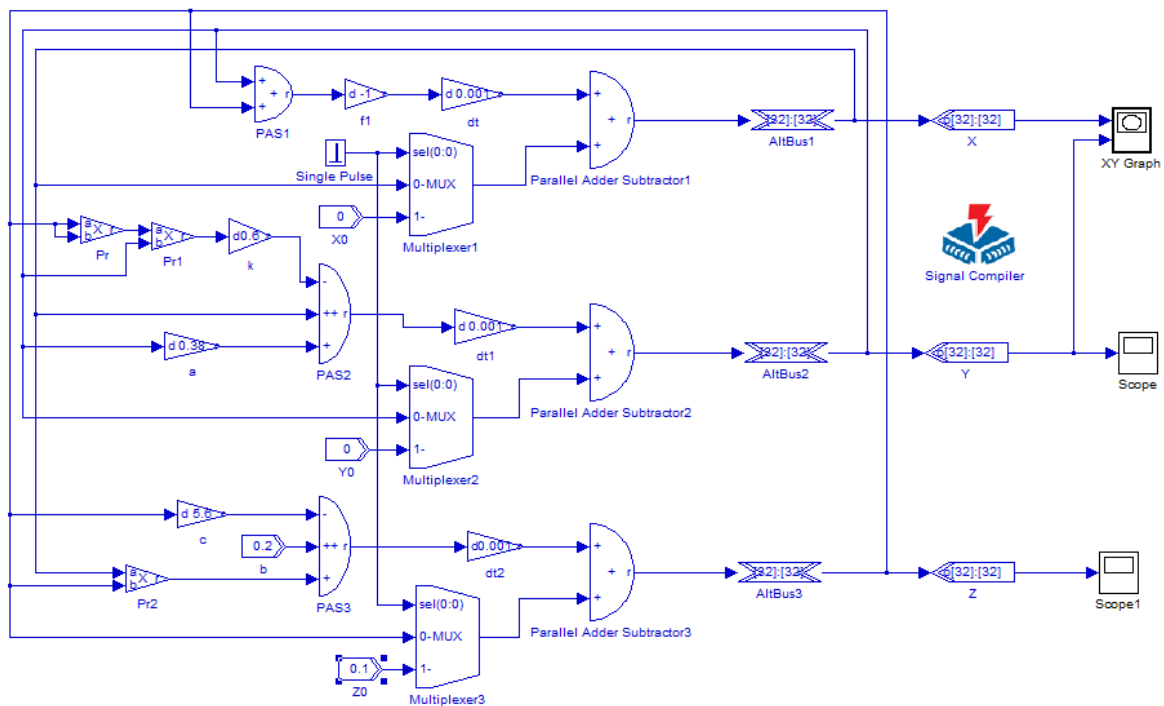


Fig. 11 Circuit realizing hidden attractors in the Simulink by DSP builder blocks

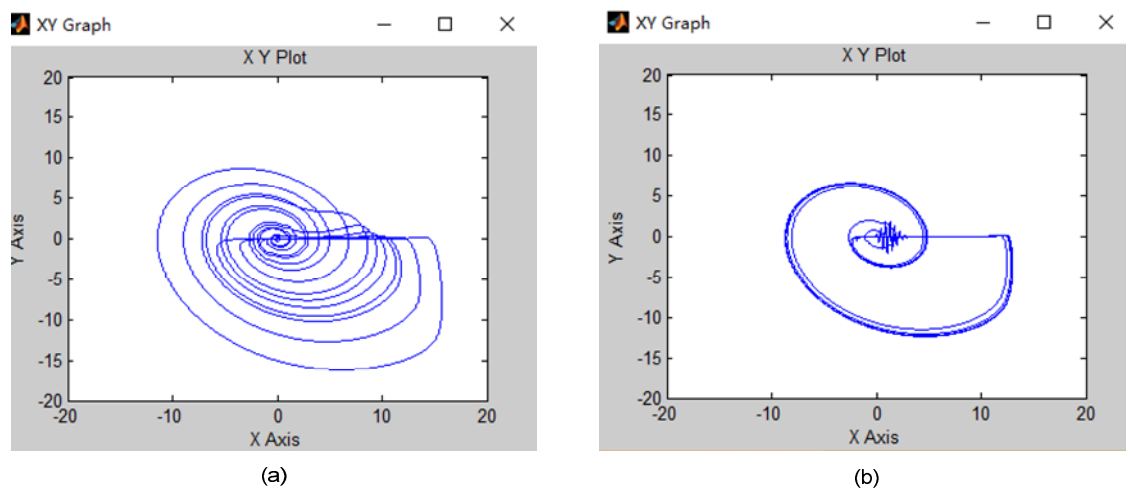


Fig. 12 An FPGA circuit-based attractor for an oscillator with a memory effect was confirmed by DSP builder. The initial values were set as (a) $z_0=0.1$, (b) $z_0=-3.3$. The parameters were set as $a=0.38$, $b=0.2$, $c=5.6$, and $k=0.6$

(Vivado) System Generator tool box which is used to generate an infinite number of coexisting hidden and self-excited attractors (Tang et al., 2018).

Generic chaotic systems are sensitive to initial values, and the orbits associated with sampled time series show distinct differences even when the initial values for variables have only slight differences. When a memory effect is considered, initial value setting can also cause a distinct transition between periodical and chaotic states even when the parameters are fixed in the system with the memory function based on a memristor. A memory term composed of an initial-dependent variable is used to modulate the dynamics of an oscillator, and the formation of an attractor is highly dependent on the initial setting even when the parameters are fixed. As a result, appropriate initials for a memory variable are set to generate periodical, chaotic oscillation. The synchronization between periodical oscillators, chaotic oscillators, and periodical and chaotic oscillators has been discussed. Results indicated that synchronization on networks composed of oscillators with memory becomes difficult. As discussed in (Ma et al., 2017a), a memristor-based memory function, which is a combined nonlinear term composed of an initial-dependent variable with higher order and other variables (e.g. kx^2y and kx^2z), shows a memory effect for which the system will be dependent on the initial setting for variable x . ky^2x , ky^2z will show a distinct memory effect and the dynamics become dependent on the initial setting for variable y . Indeed, this kind of combined nonlinear term with high order just generates multi-stability in the dynamical system and thus a difference in initial selection can develop different orbits and attractor profiles. In biological areas, a sleep-wake cycle (Jin et al., 2017) shows a distinct rhythm and period that could be associated with a memory effect. Therefore, a reliable neuron model could be built to explain and understand the synchronization transition of neurons in the nervous system.

5 Conclusions

Based on an improved Rössler model with memory, in which attractor formation and oscillation are dependent on the initial settings, synchronization between two oscillators was investigated. Bifurcation

analysis and the largest Lyapunov exponent spectra were calculated to find the state dependence on the setting of initial values for variables. An FPGA circuit was proposed and the same verification was investigated by implementation in DSP builder block. Unidirectional, bidirectional coupling via one variable was used to bridge two oscillators (periodical to periodical, periodical to chaotic, and chaotic to chaotic). Complete synchronization could be reached when the coupling intensity was beyond the threshold. Interestingly, two periodical oscillators could be coupled to reach chaotic synchronization. On the other hand, a chaotic oscillator could be tamed to become periodical when one chaotic oscillator was coupled by a periodical oscillator. Furthermore, the same problem was investigated in a chain network. Complete synchronization became difficult when each oscillator on the network was considered with memory. However, heterogeneity occurs when a few oscillators with memory can activate the network to reach synchronization by generating a continuous pulse to regulate the collective response of the network. That is, diversity in initial values will trigger different oscillators (different periods and different chaotic attractors). Thus, the network is composed of non-identical oscillators, and coupling via one variable is insufficient to enhance synchronization. This raises new challenges for researchers investigating the dynamical problems associated with this class of initial-dependent systems.

References

- Anshan H, 1988. A study of the chaotic phenomena in Chua's circuit. *IEEE International Symposium on Circuits and Systems*, p.273-276.
<https://doi.org/10.1109/ISCAS.1988.14919>
- Carroll TL, Pecora LM, 1993. Synchronizing nonautonomous chaotic circuits. *IEEE Transactions on Circuits and Systems II: Analog and Digital Signal Processing*, 40(10):646-650.
<https://doi.org/10.1109/82.246166>
- Chen S, Wang D, Li C, et al., 2004. Synchronizing strict-feedback chaotic system via a scalar driving signal. *Chaos*, 14(3):539-544.
<https://doi.org/10.1063/1.1749233>
- Cheng AL, Chen YY, 2017. Analyzing the synchronization of Rössler systems—when trigger-and-reinject is equally important as the spiral motio. *Physics Letters A*, 381(42):3641-3651.
<https://doi.org/10.1016/j.physleta.2017.09.042>
- de la Fraga LG, Tlelo-Cuautle E, 2014. Optimizing the

- maximum Lyapunov exponent and phase space portraits in multi-scroll chaotic oscillators. *Nonlinear Dynamics*, 76(2):1503-1515.
<https://doi.org/10.1007/s11071-013-1224-x>
- Fixman M, 1984. Absorption by static traps: initial-value and steady-state problems. *Journal of Chemical Physics*, 81(8):3666-3677.
<https://doi.org/10.1063/1.448116>
- Friedman D, Strowbridge BW, 2003. Both electrical and chemical synapses mediate fast network oscillations in the olfactory bulb. *Neurophysiology*, 89(5):2601-2610.
<https://doi.org/10.1152/jn.00887.2002>
- Giordano R, Aloisio A, 2011. Fixed-latency, multi-gigabit serial links with Xilinx FPGAs. *IEEE Transactions on Nuclear Science*, 58(1):194-201.
<https://doi.org/10.1109/TNS.2010.2101083>
- Graubard K, Hartline DK, 1987. Full-wave rectification from a mixed electrical-chemical synapse. *Science*, 237(4814):535-537.
<https://doi.org/10.1126/science.2885921>
- Györgyi L, Field RJ, 1992. A three-variable model of deterministic chaos in the Belousov-Zhabotinsky reaction. *Nature*, 355(6363):808-810.
<https://doi.org/10.1038/355808a0>
- Heagy JF, Carroll TL, Pecora LM, 1995. Desynchronization by periodic orbits. *Physical Review E*, 52(2):R1253-R1256.
<https://doi.org/10.1103/PhysRevE.52.R1253>
- Honein T, Chien N, Herrmann G, 1991. On conservation laws for dissipative systems. *Physics Letters A*, 155(4-5):223-224.
[https://doi.org/10.1016/0375-9601\(91\)90472-K](https://doi.org/10.1016/0375-9601(91)90472-K)
- Hu G, Xiao J, Yang J, et al., 1997. Synchronization of spatio-temporal chaos and its applications. *Physical Review E*, 56(3):2738-2746.
<https://doi.org/10.1103/PhysRevE.56.2738>
- Hunt BR, Ott E, Yorke JA, 1997. Differentiable generalized synchronization of chaos. *Physical Review E*, 55(4):4029-4034.
<https://doi.org/10.1103/PhysRevE.55.4029>
- Jin W, Lin Q, Wang A, et al., 2017. Computer simulation of noise effects of the neighborhood of stimulus threshold for a mathematical model of homeostatic regulation of sleep-wake cycles. *Complexity*, Article No. 4797545.
<https://doi.org/10.1155/2017/4797545>
- Lau FCM, Tse CK, 2003. Approximate-optimal detector for chaos communication systems. *International Journal of Bifurcation and Chaos*, 13(5):1329-1335.
<https://doi.org/10.1142/S0218127403007266>
- Li C, Chen L, Aihara K, 2008. Impulsive control of stochastic systems with applications in chaos control, chaos synchronization, and neural networks. *Chaos*, 18(2):23132.
<https://doi.org/10.1063/1.2939483>
- Lin W, He Y, 2005. Complete synchronization of the noise-perturbed Chua's circuits. *Chaos*, 15(2):23705.
<https://doi.org/10.1063/1.1938627>
- Liu X, Ma G, Jiang X, et al., 2016. H_∞ stochastic synchronization for master-slave semi-Markovian switching system via sliding mode control. *Complexity*, 21(6):430-441.
<https://doi.org/10.1002/cplx.21702>
- Luo ACJ, Han RPS, 2000. The dynamics of stochastic and resonant layers in a periodically driven pendulum. *Chaos Solitons & Fractals*, 11(14):2349-2359.
[https://doi.org/10.1016/S0960-0779\(99\)00162-9](https://doi.org/10.1016/S0960-0779(99)00162-9)
- Luo ACJ, Min F, 2011. Synchronization dynamics of two different dynamical systems. *Chaos Solitons & Fractals*, 44(6):362-380.
<https://doi.org/10.1016/j.chaos.2010.12.011>
- Lv M, Wang C, Ren G, et al., 2016. Model of electrical activity in a neuron under magnetic flow effect. *Nonlinear Dynamics*, 85(3):1479-1490.
<https://doi.org/10.1007/s11071-016-2773-6>
- Ma J, Li F, Huang L, et al., 2011. Complete synchronization, phase synchronization and parameters estimation in a realistic chaotic system. *Communications in Nonlinear Science and Numerical Simulation*, 16(9):3770-3785.
<https://doi.org/10.1016/j.cnsns.2010.12.030>
- Ma J, Wu F, Ren G, et al., 2017a. A class of initials-dependent dynamical systems. *Applied Mathematics and Computation*, 298:65-76.
<https://doi.org/10.1016/j.amc.2016.11.004>
- Ma J, Mi L, Zhou P, et al., 2017b. Phase synchronization between two neurons induced by coupling of electromagnetic field. *Applied Mathematics and Computation*, 307:321-328.
<https://doi.org/10.1016/j.amc.2017.03.002>
- Ma J, Wu F, Wang C, 2017c. Synchronization behaviors of coupled neurons under electromagnetic radiation. *International Journal of Modern Physics B*, 31(2):1650251.
- Mahmoud GM, Mahmoud EE, 2010. Complete synchronization of chaotic complex nonlinear systems with uncertain parameters. *Nonlinear Dynamics*, 62(4):875-882.
<https://doi.org/10.1007/s11071-010-9770-y>
- Mankin R, Laas K, Laas T, et al., 2018. Memory effects for a stochastic fractional oscillator in a magnetic field. *Physical Review E*, 97(1):12145.
<https://doi.org/10.1103/PhysRevE.97.012145>
- Martinet B, Adrian RJ, 1988. Rayleigh-Benard convection: experimental study of time-dependent instabilities. *Experiments in Fluids*, 6(5):316-322.
<https://doi.org/10.1007/BF00538822>
- Osipov GV, Pikovsky AS, Kurths J, 2002. Phase synchronization of chaotic rotators. *Physical Review Letters*, 88(4):54102.
<https://doi.org/10.1103/PhysRevLett.88.054102>
- Pano-Azucena AD, Rangel-Magdaleno JJ, Tlelo-Cuautle E, et al., 2017. Arduino-based chaotic secure communication system using multi-directional multi-scroll chaotic oscillators. *Nonlinear Dynamics*, 87(4):2203-2217.
<https://doi.org/10.1007/s11071-016-3184-4>

- Pecora LM, Carroll TL, 2015. Synchronization of chaotic systems. *Chaos*, 25(9):97611.
<https://doi.org/10.1063/1.4917383>
- Pena Ramirez J, Fey RHB, Nijmeijer H, 2013. Synchronization of weakly nonlinear oscillators with Huygens' coupling. *Chaos*, 23(3):33118.
<https://doi.org/10.1063/1.4816360>
- Peng JH, Ding EJ, Ding M, et al., 1996. Synchronizing hyperchaos with a scalar transmitted signal. *Physical Review Letters*, 76(6):904-907.
<https://doi.org/10.1103/PhysRevLett.76.904>
- Pereda AE, 2014. Electrical synapses and their functional interactions with chemical synapses. *Nature Reviews Neuroscience*, 15:250-263.
<https://doi.org/10.1038/nrn3708>
- Podvigina NF, Bagaeva TV, Podvigina DN, et al., 2008. Selective self-synchronization of impulse flows in neuronal networks of the visual system. *Biophysics*, 53(2):177-181.
<https://doi.org/10.1134/S0006350908020097>
- Rössler OE, 1976. An equation for continuous chaos. *Physics Letters A*, 57(5):397-398.
[https://doi.org/10.1016/0375-9601\(76\)90101-8](https://doi.org/10.1016/0375-9601(76)90101-8)
- Ruggieri M, Speciale MP, 2017. On the construction of conservation laws: a mixed approach. *Journal of Mathematical Physics*, 58(2):23510.
<https://doi.org/10.1063/1.4976189>
- Sieberer LM, Huber SD, Altman E, et al., 2013. Dynamical critical phenomena in driven-dissipative systems. *Physical Review Letters*, 110(19):195301.
<https://doi.org/10.1103/PhysRevLett.110.195301>
- Szot P, 2012. Common factors among Alzheimer's disease, Parkinson's disease, and epilepsy: possible role of the noradrenergic nervous system. *Epilepsia*, 53(S1):61-66.
<https://doi.org/10.1111/j.1528-1167.2012.03476.x>
- Tang YX, Khalaf AJM, Rajagopal K, et al., 2018. A new nonlinear oscillator with infinite number of coexisting hidden and self-excited attractors. *Chinese Physics B*, 27(4):40502.
<https://doi.org/10.1088/1674-1056/27/4/040502>
- Tlelo-Cuautle E, Carbajal-Gomez VH, Obeso-Rodelo PJ, et al., 2015a. FPGA realization of a chaotic communication system applied to image processing. *Nonlinear Dynamics*, 82(4):1879-1892.
<https://doi.org/10.1007/s11071-015-2284-x>
- Tlelo-Cuautle E, Rangel-Magdaleno JJ, Pano-Azucena AD, et al., 2015b. FPGA realization of multi-scroll chaotic oscillators. *Communications in Nonlinear Science and Numerical Simulation*, 27(1-3):66-80.
<https://doi.org/10.1016/j.cnsns.2015.03.003>
- Tlelo-Cuautle E, Rangel-Magdaleno J, de la Fraga LG, 2016a. Engineering Applications of FPGAs: Chaotic Systems, Artificial Neural Networks, Random Number Generators, and Secure Communication Systems. Springer, Cham, Switzerland.
<https://doi.org/10.1007/978-3-319-34115-6>
- Tlelo-Cuautle E, Pano-Azucena AD, Rangel-Magdaleno JJ, et al., 2016b. Generating a 50-scroll chaotic attractor at 66 MHz by using FPGAs. *Nonlinear Dynamics*, 85(4):2143-2157.
<https://doi.org/10.1007/s11071-016-2820-3>
- Tlelo-Cuautle E, de Jesus Quintas-Valles A, de la Fraga LG, et al., 2016c. VHDL descriptions for the FPGA implementation of PWL-function-based multi-scroll chaotic oscillators. *PLoS ONE*, 11(2):e0168300.
<https://doi.org/10.1371/journal.pone.0168300>
- Tlelo-Cuautle E, de la Fraga LG, Pham VT, et al., 2017. Dynamics, FPGA realization and application of a chaotic system with an infinite number of equilibrium points. *Nonlinear Dynamics*, 89(2):1129-1139.
<https://doi.org/10.1007/s11071-017-3505-2>
- Trejo-Guerra R, Tlelo-Cuautle E, Jiménez-Fuentes JM, et al., 2012. Integrated circuit generating 3- and 5-scroll attractors. *Communications in Nonlinear Science and Numerical Simulation*, 17(11):4328-4335.
<https://doi.org/10.1016/j.cnsns.2012.01.029>
- Trejo-Guerra R, Tlelo-Cuautle E, Carbajal-Gomez VH, et al., 2013. A survey on the integrated design of chaotic oscillators. *Applied Mathematics and Computation*, 219(10):5113-5122.
<https://doi.org/10.1016/j.amc.2012.11.021>
- Ueda Y, Akamatsu N, 1981. Chaotically transitional phenomena in the forced negative-resistance oscillator. *IEEE Transactions on Circuits and Systems*, 28(3):217-224.
<https://doi.org/10.1109/TCS.1981.1084975>
- Vaidyanathan S, Volos C, 2016. Advances and Applications in Chaotic Systems. Springer, Cham, Switzerland.
<https://doi.org/10.1007/978-3-319-30279-9>
- Vyas S, Huang H, Gale JT, et al., 2016. Neuronal complexity in subthalamic nucleus is reduced in Parkinson's disease. *IEEE Transactions Neurology System Rehabilitation Engineering*, 24(1):36-45.
<https://doi.org/10.1109/TNSRE.2015.2453254>
- Wang C, Ma J, 2018. A review and guidance for pattern selection in spatiotemporal system. *International Journal of Modern Physics B*, 32(6):1830003.
- Wang G, Jin W, Liu H, et al., 2018. The synchronization of asymmetric-structured electric coupling neuronal system. *International Journal of Modern Physics B*, 32(4):1850040.
- Wang H, Wang Q, Lu Q, 2011. Bursting oscillations, bifurcation and synchronization in neuronal systems. *Chaos Solitons & Fractals*, 44(8):667-675.
<https://doi.org/10.1016/j.chaos.2011.06.003>
- Wang Y, Ma J, Xu Y, et al., 2017. The electrical activity of neurons subject to electromagnetic induction and Gaussian white noise. *International Journal of Bifurcation and Chaos*, 27(2):1750030.
<https://doi.org/10.1142/S0218127417500304>
- Wu F, Wang C, Xu Y, et al., 2016. Model of electrical activity in cardiac tissue under electromagnetic induction. *Science*

Reports, 6(1):28.

<https://doi.org/10.1038/s41598-016-0031-2>

Wu F, Wang C, Jin W, et al., 2017. Dynamical responses in a new neuron model subjected to electromagnetic induction and phase noise. *Physica A: Statistical Mechanics and Its Applications*, 469:81-88.

<https://doi.org/10.1016/j.physa.2016.11.056>

Xu Y, Ying H, Jia Y, et al., 2017. Autaptic regulation of electrical activities in neuron under electromagnetic induction. *Science Reports*, 7:43452.

<https://doi.org/10.1038/srep43452>

Yamada T, Fujisaka H, 1986. Intermittency caused by chaotic modulation. I: Analysis with a multiplicative noise model. *Progress of Theoretical Physics*, 76(3):582-591.

<https://doi.org/10.1143/PTP.76.582>

Yang SS, Duan CK, 1998. Generalized synchronization in chaotic systems. *Chaos Solitons & Fractals*, 9(10):1703-1707.

[https://doi.org/10.1016/S0960-0779\(97\)00149-5](https://doi.org/10.1016/S0960-0779(97)00149-5)

Yang T, Yang LB, Yang CM, 1997. Impulsive control of Lorenz system. *Physica D: Nonlinear Phenomena*, 110(1-2):18-24.

[https://doi.org/10.1016/S0167-2789\(97\)00116-4](https://doi.org/10.1016/S0167-2789(97)00116-4)

Zhang XH, Liu SQ, 2018. Stochastic resonance and synchronization behaviors of excitatory-inhibitory small-world network subjected to electromagnetic induction. *Chinese Physics B*, 27(4):40501.

<https://doi.org/10.1088/1674-1056/27/4/040501>

中文概要

题目: 初始值敏感的周期和混沌振荡模态系统同步稳定性

目的: 具有记忆特性的振子系统的模态选择对初始值具有敏感性。本文旨在探讨初始值控制的振子的耦合同步稳定一致性问题。

创新点: 1. 两个周期振子耦合后达到混沌同步; 2. 周期振子和混沌振子耦合后达到周期性振荡同步。

方法: 1. 通过分岔分析, 研究振荡模态和初始值选择之间的关系 (图 2、6 和 8); 2. 通过数值计算, 研究两个周期振子在耦合下的混沌同步关系 (图 7); 3. 通过计算同步因子和斑图, 分析同步一致性对耦合强度与记忆函数增益的依赖程度 (图 9 和 10); 4. 通过现场可编程门阵列验证动力系统模态对初始值的依赖程度 (图 11 和 12)。

结论: 1. 具有记忆函数的非线性振子的动力学行为 (如吸引子) 在参数固定的情况下与初始值选取有关。2. 不同类型振子的耦合可以达到多样同步行为; 周期振子耦合达到混沌同步; 周期振子耦合混沌振子可以抑制混沌。3. 包含记忆函数的振子网络耦合同步非常困难。

关键词: 同步; 分岔; 同步因子; 现场可编程门阵列